

## **General Disclaimer**

### **One or more of the Following Statements may affect this Document**

- This document has been reproduced from the best copy furnished by the organizational source. It is being released in the interest of making available as much information as possible.
- This document may contain data, which exceeds the sheet parameters. It was furnished in this condition by the organizational source and is the best copy available.
- This document may contain tone-on-tone or color graphs, charts and/or pictures, which have been reproduced in black and white.
- This document is paginated as submitted by the original source.
- Portions of this document are not fully legible due to the historical nature of some of the material. However, it is the best reproduction available from the original submission.

**NASA TECHNICAL  
MEMORANDUM**

**NASA TM X- 73985**

**NASA TM X- 73985**

(NASA-TM-X-73985) THE ACOUSTIC MONOPOLE IN  
MOTION (NASA) 28 p HC A03/MF A01 CSCL 20A

N77-11816

Unclas  
G3/71 54511

**THE ACOUSTIC MONOPOLE IN MOTION**

By

Thomas D. Norum

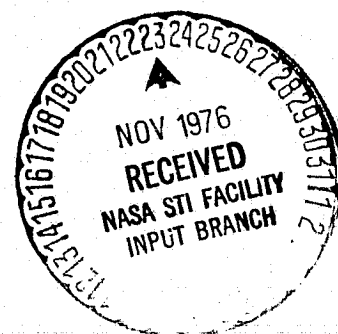
and

Chen-Huei Liu

November 1976

This informal documentation medium is used to provide accelerated or special release of technical information to selected users. The contents may not meet NASA formal editing and publication standards, may be revised, or may be incorporated in another publication.

**NATIONAL AERONAUTICS AND SPACE ADMINISTRATION  
LANGLEY RESEARCH CENTER, HAMPTON, VIRGINIA 23665**



Report No. NASA TM X-73985		2. Government Accession No.		3. Recipient's Catalog No.	
4. Title and Subtitle The Acoustic Monopole in Motion				5. Report Date November 1976	
				6. Performing Organization Code 2620	
7. Author(s) Thomas D. Norum and Chen-Huei Liu				8. Performing Organization Report No. TM X-73985	
9. Performing Organization Name and Address NASA Langley Research Center Hampton, Virginia 23665				10. Work Unit No. 505-03-11-02	
				11. Contract or Grant No.	
12. Sponsoring Agency Name and Address National Aeronautics and Space Administration Washington, D. C. 20546				13. Type of Report and Period Covered Technical Memorandum	
				14. Sponsoring Agency Code	
15. Supplementary Notes Material to be presented at the 92nd ASA Meeting to be held in San Diego, CA November 16-19, 1976					
16. Abstract A widely used experimental version of the acoustic monopole consists of an acoustic driver of restricted opening forced by a discrete frequency oscillator. To investigate the effects of forward motion on this source, it was mounted above an automobile and driven over an asphalt surface at constant speed past a microphone array. Shapes of the received signal were compared to results computed from an analysis of a fluctuating mass type point source moving above a finite impedance reflecting plane. Good agreement was found between experiment and theory when a complex normal impedance representative of a fairly hard acoustic surface was used in the analysis. Nonuniform motion of the source was also considered by analyzing the monopole moving with constant linear acceleration in free space. Computation of the observed signal indicates that deviations from the constant velocity case may be significant only at rather large values of acceleration.					
17. Key Words (Suggested by Author(s)) Acoustic monopole, moving source, ground reflections				18. Distribution Statement Unclassified - Unlimited	
19. Security Classif. (of this report) UNCLASSIFIED		20. Security Classif. (of this page) UNCLASSIFIED		22. Price* \$3.75	
				21. No. of Pages 26	

## ABSTRACT

A widely used experimental version of the acoustic monopole consists of an acoustic driver of restricted opening forced by a discrete frequency oscillator. To investigate the effects of forward motion on this source, it was mounted above an automobile and driven over an asphalt surface at constant speed past a microphone array. The shapes of the received signal were compared to results computed from an analysis of a fluctuating mass type point source moving above a finite impedance reflecting plane. Good agreement was found between experiment and theory when a complex normal impedance representative of a fairly hard acoustic surface was used in the analysis. Nonuniform motion of the source was also considered by analyzing the monopole moving with constant linear acceleration in free space. Computation of the observed signal indicates that deviations from the constant velocity case may be significant only at rather large values of acceleration.

## INTRODUCTION

Over the past few years, a considerable effort has been made by many investigators to understand the effect of source motion on noise generation and propagation. Information on some of these effects can be obtained by looking at the simplest of noise sources, the point monopole. This report presents the results of an experiment in which a small monochromatic source, which behaves like an acoustic monopole

when stationary, is moved at a constant speed over an asphalt surface past stationary microphones. Also reported is an analysis of the monopole moving above a finite impedance reflecting plane. The theoretical and experimental results are compared for different ground to observer heights, source frequencies, and source velocities. A computation of the effects of source acceleration on the noise radiated by the monopole is also presented.

### SYMBOLS

Measurements and calculations were made in U. S. Customary Units. This paper presents physical quantities in the International System of Units (SI) with the equivalent values in U. S. Customary Units given parenthetically.

- a - source acceleration
- A, B, D parameters defined in equation (20)
- c - speed of sound in air
- $C_R$  - reflection coefficient
- $\overline{C}_R$  - reflection coefficient in Fourier transformed Lorentz space
- F - source frequency
- g - acceleration due to gravity
- h - distance between source and reflecting plane
- k - wave number,  $\omega/c$
- $K_j$  - wave number components in transformed Lorentz space
- M - source Mach number,  $U/c$
- p - acoustic pressure
- q - source strength function

- $q_0$  - magnitude of source strength
- $r$  - source to observer distance
- $R$  - convection modified source to observer distance (eq. 12a)
- $s$  - source position function
- $t$  - time
- $U$  - source velocity
- $x, y, z$  cartesian coordinates
- $y_0, z_0$  observer coordinates
- $Z$  - ratio of normal impedance to characteristic impedance of air,  $\zeta/\rho c$ .
- $\gamma$  -  $(1 - M^2)^{-1/2}$
- $\delta$  - Dirac delta function
- $\zeta$  - normal impedance of reflecting plane
- $\theta$  - angle between direction of motion and line joining source to observer.
- $\rho$  - density of air
- $\sigma$  - source to observer distance at closest approach
- $\tau$  - retarded time
- $\psi$  - acoustic velocity potential
- $\omega$  - angular frequency
- $\nabla^2$  - Laplacian operator
- $\square^2$  - wave operator

Subscript L denotes Lorentz space

Prime (') denotes derivative with respect to retarded time,  $t-r/c$

## EXPERIMENT

The experimental source was similar in design to that used in other investigations (1, 2, 3). It consisted of a 60 watt acoustic driver necked down to a 1.52 cm (1/2 in.) diameter tubular opening. When driven by an oscillator at a discrete frequency, the output of this source consists of tones at the oscillator frequency and its harmonics. By appropriate filtering, the measured signal consists essentially of a discrete frequency.

This source possesses the well-known characteristic of radiating approximately uniformly in all directions in a stationary medium as long as the wave length of the sound is considerably larger than the tube diameter. Since its physical operation consists of a time rate of introduction of mass, it corresponds to an acoustic monopole.

Although the radiation pattern of the experimental source in a stationary medium is easily measured, its behavior when relative motion exists between the medium and the source is not readily determined. It has been assumed by previous investigators (1,3) that the generation characteristics are unchanged by this motion. Hence an experiment was designed to test the assumption that the source does radiate in the expected manner. This experiment deals with the effects of motion on source directivity changes rather than on source output level changes.

The source was positioned 7.9 m (26 ft.) from the ground above an automobile via a guy wire supported mast (fig. 1). An oscillator

located in the trunk of the vehicle excited the source at a frequency of either 1230 Hz or 2310 Hz. The automobile was driven at constant speeds ranging from 13.4 to 44.7 m/s (30 to 100 mph) which were recorded on a strip chart within the vehicle. Sideline microphones were located at a closest approach distance of 11.0 m (36 ft.) and positioned 3.05 m (10 ft.) and 6.10 meters (20 ft.) from the ground surface. The experiment was performed on an aircraft runway consisting of a 16.5 cm (6.5 in.) asphalt surface on top of a concrete foundation. Figure 2 gives a schematic of the experimental setup.

The pressure signals were measured with 1.3 cm diameter (1/2 in.) condenser microphones and recorded on magnetic tape. In both the recording and reproduction stages the data were passed through a band pass filter set to pass all the frequency components possible due to the Doppler effect on the oscillator frequency. The analog tapes were digitized at the rate of 10,000 points per second.

The oscillator frequency was set to an accuracy of  $\pm 1$  Hz. Vehicle speed varied by no more than  $\pm 0.5$  m/s ( $\pm 1$  mph) over the test zone. The frequency response of the recording and analysis system was estimated to be flat within  $\pm 0.5$  dB over all frequencies of interest.

#### ANALYSIS OF A MONOPOLE WITH CONSTANT VELOCITY ABOVE A FINITE IMPEDANCE REFLECTING PLANE

For the monopole of angular frequency  $\omega$  and strength  $q_0$  moving with constant velocity  $U$  in the  $x$  direction at a distance  $h$  above the  $x$ - $z$  plane (fig. 3), the propagation is governed by:



$$\square^2 \psi(x, y, z, t) = -q_0 e^{-i\omega t} \delta(x-Ut) \delta(y-h) \delta(z) \quad (1)$$

where  $\square^2$  is the wave operator,  $\nabla^2 - \frac{1}{c^2} \frac{\partial^2}{\partial t^2}$ , and  $\psi$  is the acoustic velocity potential. Specifying the x-z plane to be a locally reacting surface of normal impedance  $\zeta$ , the velocity potential must satisfy the condition:

$$\left( \frac{1}{c} \frac{\partial}{\partial t} - Z \frac{\partial}{\partial y} \right) \psi(x, y, z, t) = 0 \quad \text{at } y = 0 \quad (2)$$

where

$$Z = \zeta / \rho c.$$

The equivalent stationary problem is obtained by utilizing the Lorentz transformation:

$$\begin{aligned} x_L &= \gamma^2 (x - Mct) \\ y_L &= \gamma y \\ z_L &= \gamma z \\ t_L &= \gamma^2 (t - \frac{M}{c}x) \end{aligned} \quad (3)$$

where  $M = U/c$  and  $\gamma = (1-M^2)^{-1/2}$ . This transformation reduces (1) to

$$\square_L^2 \psi(x_L, y_L, z_L, t_L) = -\gamma^2 q_0 e^{-i\omega t_L} \delta(x_L) \delta(y_L - h_L) \delta(z_L) \quad (4)$$

where  $h_L = \gamma h$ , and the boundary condition to

$$\left( \frac{1}{c} \frac{\partial}{\partial t_L} - M \frac{\partial}{\partial x_L} - \frac{Z}{\gamma} \frac{\partial}{\partial y_L} \right) \psi(x_L, y_L, z_L, t_L) = 0 \quad \text{at } y_L = 0 \quad (5)$$

Utilizing a Fourier transformation on the spacial variables a solution to (4) is easily shown to be

$$\psi(x_L, y_L, z_L, t_L) = \frac{\gamma^2 q_0 e^{-i\omega t_L}}{(2\pi)^3} \iiint_{-\infty}^{\infty} \frac{dK_1 dK_2 dK_3 e^{-i(K_1 x_L + K_2(y_L - h_L) + K_3 z_L)}}{K_1^2 + K_2^2 + K_3^2 - k^2} \quad (6)$$

where  $k = \omega/c$  and the  $K_j$  are the wave number components in the coordinate directions of the transformed Lorentz space. This solution corresponds to a decomposition of the radiation from a point source located at  $(0, h_L, 0)$  in Lorentz space into a system of plane waves represented by the exponential of the integrand. To satisfy the boundary condition (5) a system of waves corresponding to an image source at  $(0, -h_L, 0)$  and modified by a reflection coefficient,  $\bar{C}_R$ , is added to this solution. The total field is then given by

$$\psi(x_L, y_L, z_L, t_L) = \frac{\gamma^2 q_0 e^{-i\omega t_L}}{(2\pi)^3} \iiint_{-\infty}^{\infty} \frac{dK_1 dK_2 dK_3}{K_1^2 + K_2^2 + K_3^2 - k^2} \times$$

$$\times \left[ e^{-i(K_1 x_L + K_2(y_L - h_L) + K_3 z_L)} + \bar{C}_R e^{-i(K_1 x_L - K_2(y_L + h_L) + K_3 z_L)} \right] \quad (7)$$

Substituting this into the boundary condition gives the reflection coefficient as:

$$\bar{C}_R = \frac{Z \frac{K_2}{k} - \gamma(1 - M \frac{K_1}{k})}{Z \frac{K_2}{k} + \gamma(1 - M \frac{K_1}{k})} \quad (8)$$

Equations (7) and (8) give the exact solution for the velocity potential in the Lorentz coordinates. The first term in the brackets corresponds

to the direct radiation from the source and is easily evaluated. However, the second term, representing radiation from the image source modified by the reflection coefficient, cannot be evaluated analytically. Hence, an approximation is obtained in a manner analogous to that presented in reference 4 (page 371). This approximation will be valid as long as the observer is not closer than a half wavelength to the surface. Noting that  $K_j/k$  corresponds to the cosine of the angle between the  $j$ -axis and the line from the image to the observer, the approximation for the velocity potential is:

$$\psi(x_L, y_L, z_L, t_L) \approx \frac{\gamma^2 q_0 e^{-i\omega t_L}}{4\pi} \left( \frac{e^{ikr_1}}{r_1} + C_R \frac{e^{ikr_2}}{r_2} \right) \quad (9)$$

where

$$\begin{aligned} r_1 &= [x_L^2 + (y_L - h_L)^2 + z_L^2]^{1/2} \\ r_2 &= [x_L^2 + (y_L + h_L)^2 + z_L^2]^{1/2} \\ C_R &= \frac{z \frac{x_L}{r_2} - \gamma (1 - M \frac{y_L + h_L}{r_2})}{z \frac{x_L}{r_2} + \gamma (1 - M \frac{y_L + h_L}{r_2})} \end{aligned} \quad (10)$$

Transforming back into the physical plane and specifying the observer to be located at  $(0, y_0, z_0)$  gives

$$\psi(0, y_0, z_0, t) \approx \frac{q_0}{4\pi} \left( \frac{e^{-i\omega\gamma^2(t-R_1/c)}}{R_1} + C_R \frac{e^{i\omega\gamma^2(t-R_2/c)}}{R_2} \right) \quad (11)$$

where

$$R_1 = \left[ (Mct)^2 + \left( \frac{y_0 - h}{\gamma} \right)^2 + \left( \frac{z_0}{\gamma} \right)^2 \right]^{1/2} \quad (12a)$$

$$R_2 = \left[ (Mct)^2 + \left( \frac{y_0+h}{\gamma} \right)^2 + \left( \frac{z_0}{\gamma} \right)^2 \right]^{1/2} \quad (12b)$$

$$C_R = \frac{z(y_0+h) - \gamma^2 (R_2 + M^2 ct)}{z(y_0+h) + \gamma^2 (R_2 + M^2 ct)} \quad (12c)$$

Note that if the Mach number is set equal to zero the reflection coefficient reduces to

$$C_R = \frac{z \frac{y_0+h}{R_2} - 1}{z \frac{y_0+h}{R_2} + 1} \quad (13)$$

which is the result one obtains for a stationary source. Hence, the effect of source motion is to introduce a convection term into the reflection coefficient. This convection term in equation (12) is seen to be more important for small values of impedance and small incidence angles ( $R_2 \gg y_0+h$ ), and increases in significance as the source velocity increases.

The acoustic pressure is obtained in the usual manner from the velocity potential by

$$p(0, y_0, z_0, t) = -\rho \frac{\partial \psi(0, y_0, z_0, t)}{\partial t} \quad (14)$$

#### ANALYSIS OF THE POINT SOURCE IN LINEAR MOTION IN FREE SPACE

To determine the extent of acceleration effects, linear source motion in the absence of a reflecting plane was considered.

The propagation of sound from a point source moving with arbitrary velocity along the x-axis is governed by

$$\square^2 \psi(x, y, z, t) = - q(t) \delta(x-s(t)) \delta(y) \delta(z) \quad (15)$$

where  $s(t)$  is the source position function. The free space solution is easily obtained by the procedure described by Lowson (5) as

$$\psi = \frac{q}{4\pi r (1 - M \cos \theta)} \quad (16)$$

where each of the variables  $q$ ,  $r$ ,  $M$ , and  $\theta$  are evaluated at the retarded time  $t - r/c$ . Here  $r$  is the source to observer distance,  $M$  is the instantaneous Mach number, and  $\theta$  is the angle between the direction of motion and the line joining source to observer.

Solving the acoustic pressure from equation (14) yields:

$$p = - \frac{\rho}{4\pi r (1 - M \cos \theta)^2} \left[ q' + q \frac{M' \cos \theta}{(1 - M \cos \theta)} + q \frac{M c (\cos \theta - M)}{r (1 - M \cos \theta)} \right] \quad (17)$$

where the primes denote derivatives with respect to retarded time and again all variables are evaluated at this time.

This solution is equivalent to the result given by Lowson (5) for the solution to the wave equation for perturbation density of a moving source representing a single time rate of introduction of mass. This equivalence is readily seen by a time differentiation of equation (5). (A good description of the subtleties in the mathematical specification of moving point sources is given in reference (5).

For a discrete frequency the source function becomes:

$$q(t) = q_0 e^{-i\omega t} \quad (18)$$

Evaluating the rms value of the pressure from (17) and normalizing by the rms pressure due to this same source radiating at the constant distance  $\sigma$  from the observer yields

$$\frac{p_{rms}}{p_{rms\_stationary}} = \frac{\sin\theta}{(1-M\cos\theta)^2} (1 + B^2)^{1/2} \quad (19)$$

where

$$\begin{aligned} B &= A + D \\ &= \frac{M' \cos\theta}{\omega(1-M\cos\theta)} + \frac{cM \sin\theta(\cos\theta-M)}{\omega\sigma(1-M\cos\theta)} \end{aligned} \quad (20)$$

For a constant acceleration,  $a$ , of the source,

$$M' = a/c \quad (21)$$

It is evident that  $A$  is zero for the constant velocity source whereas  $D$  is zero only for the stationary source. To determine the significance of  $B$  in (19), let the parameters to be restricted to conditions that include most cases of practical interest as follows:

$$\sigma \geq 10 \text{ m}$$

$$\frac{\omega}{2\pi} \geq 50 \text{ Hz} \quad (22)$$

$$M \leq 0.9$$

$$a \leq 10 \text{ g}$$

Then, using  $c = 340 \text{ m/s}$ ,

$$|A| = \left| \frac{a \cos\theta}{c\omega(1-M\cos\theta)} \right| \leq \left| \frac{a}{c\omega(1-M)} \right| < 0.01$$

$$|B| = \left| \frac{cM \sin\theta(\cos\theta-M)}{\omega\sigma(1-M\cos\theta)} \right| \leq \left| \frac{cM}{\omega\sigma} \right| < 0.10$$

Hence

$$(1 + B^2)^{1/2} \leq \left[ 1 + (|A| + |D|)^2 \right]^{1/2} < 1.01$$

Thus, under the conditions (22), the effects of motion of the source on the observed pressure can be represented to within an error of less than 1 percent by

$$\frac{p_{rms}}{p_{rms\_stationary}} = \frac{\sin\theta}{(1-M\cos\theta)^2} \quad (23)$$

### RESULTS

To investigate the effects of motion on the experimental point source and the extent to which the observed signal can be predicted analytically, various comparisons of the time histories were made. These comparisons are shown in figures 4-9, in which the mean square pressure in dB is plotted against the normalized time  $Ut/\sigma$ , where  $U$  is the source velocity and  $\sigma$  is the closest approach distance. The analytical mean square pressure was computed at discrete points in time from equation (14), whereas the experimental values were obtained by averaging the digitized data over a time interval corresponding to a given increment in the source travel distance. The comparisons below include the effect of analysis time on the perceived results, the effects of varying source frequency, source velocity, and observer height, and the dependence of the computed results on ground impedance.

To see the effect of analysis time on the observed signal, one of the experimental time histories was analyzed using three different analysis times. In figure 4a, each plotted point corresponds to 1.52 centimeter of source travel distance (1.52 cm/point), whereas 10.7 cm/point and 152 cm/point were used in figures 4b and 4c, respectively. Each of the first two curves show the pattern of alternate reinforcements and

cancellations caused by the reflected wave, although the magnitudes of the cancellations are seen to differ by as much as 10 dB between the two curves. (The same phenomena was obtainable with the theoretical results when different time intervals between computed points were used.) This not unexpected fact illustrates that little information about the reflected wave from an acoustically hard surface can be obtained from a consideration of the magnitude of the cancellations. Figure 4c shows that the details of the reflection process are lost if the analysis time is not chosen small enough.

A comparison of the theoretical and experimental results is given in figure 5. The time interval between computed points for all the theoretical curves presented was chosen to correspond to 10.7 cm/point. Superimposed on each of these curves is the signal that would be received in the absence of the ground surface, obtained by using a value of zero for the reflection coefficient. The value chosen for the normalized ground impedance in the theoretical curve of figure 5 was  $Z = 4 - i4$ , a value indicative of a fairly hard ground surface. One can see a good agreement between the curves both in shape and in the time intervals between the alternate reinforcements and cancellations.

Computations showing the effect on the observed signal due to varying ground impedance are given in figure 6. The two curves show the fact that the magnitude of the reinforcements and cancellations increase with the magnitude of the ground impedance. Although not shown here, computations using smaller values of impedance give the same



trend, with some minor variations in the shape of the signal at very small impedance. However, the differences in the computed results are not significant enough to enable a quantitative determination of the impedance of the experimental surface by comparison of experiment and theory.

Figures 7 and 8 show the effect of varying ground to observer distance and source frequency, respectively. Decreases in the time interval between successive reinforcements and cancellations are seen to occur in both the theoretical and experimental results with increasing ground to observer distance and increasing frequency.

The effect of source velocity can be seen in figure 9. Since the time axis has been normalized by using the velocity, the shapes of the observed signal are the same. (The erratic nature of the experimental curves with increasing velocity is due to a smaller analysis time being used as the velocity increases.)

Many of the above results are qualitatively predictable from a simple consideration of the time and length scales involved. The purpose of the comparisons presented is to show the good agreement in the shapes of the experimental and theoretical results. This agreement gives credence to the assumption that the experimental source indeed radiates in the same manner as a theoretical monopole in motion.

The effects on the observed signal due to constant linear acceleration of the theoretical monopole were determined from equation (23). Figure 10 gives the observed pressure vs. the source to observer angle at the emission time for a Mach number at closest approach equal to 0.9. The maximum differences from the constant

velocity case correspond to about 3 dB at an acceleration of  $10g$  and less than 0.5 dB at an acceleration of  $1g$ . These maximum differences are found to be half these amounts for a closest approach Mach number of 0.3.

### CONCLUSIONS

Effects of forward motion on acoustic generation and propagation were investigated using a point monochromatic source. An experimental source, which radiates like the theoretical monopole when in a stationary environment, was put into motion and comparisons were made between its acoustic radiation and that of the moving theoretical monopole. The effects of source acceleration were also considered in the analytical investigation. The following conclusions can be made from the results:

1. The comparisons of the shapes of the measured and computed pressure signals indicate that the experimental source does retain its monopole characteristics when relative motion exists between it and the surrounding medium.
2. The magnitude of the cancellations due to interference between the direct and reflected waves is very sensitive to the time interval used in the analysis. Hence, little information about the reflected wave from an acoustically hard surface can be obtained from a consideration of these cancellation magnitudes. Although the results are for a discrete frequency source, the same conclusion applies to narrow band analysis of nonstationary random noise.
3. The theoretical analysis of the monopole moving at constant velocity yields a convection term in the relationship between the reflection

coefficient and ground impedance. This modification to the reflection coefficient of the stationary case is seen to grow in importance with increasing source velocity and incidence angle.

4. Computations of the observed signal from a theoretical monopole accelerating at subsonic speed show that differences from the constant velocity case become significant only at rather large values of acceleration. Hence, in most practical situations, the effects of acceleration on the received signal can be neglected.

#### REFERENCES

1. Atvars, J.; Shubert, L. K.; Grande, E.; and Ribner, H. S.: Refraction of Sound by Jet Flow and Jet Temperature. NASA CR 494, May 1966.
2. Norum, T. D.: Measured and Calculated Transmission Losses of Sound Waves Through a Helium Layer. NASA TN D-7230, May 1973.
3. Maestrello, L: On the Relationship Between Acoustic Energy Density Flux Near the Jet and Far-Field Acoustic Intensity, AIAA Paper No. 73-988, October 1973.
4. Morse, P. M.; and Ingard, K. U.: Theoretical Acoustics. McGraw Hill, 1968.
5. Lowson, M. V.: The Sound Field for Singularities in Motion. Royal Society of London, Proceedings Series A, vol. 286, August 1965, pages 559-572.
6. Warren, C. H. E.: A Note on Moving Multipole Sources of Sound. Journal of Sound and Vibration, vol. 44, no. 1, 1976, pages 3-13.

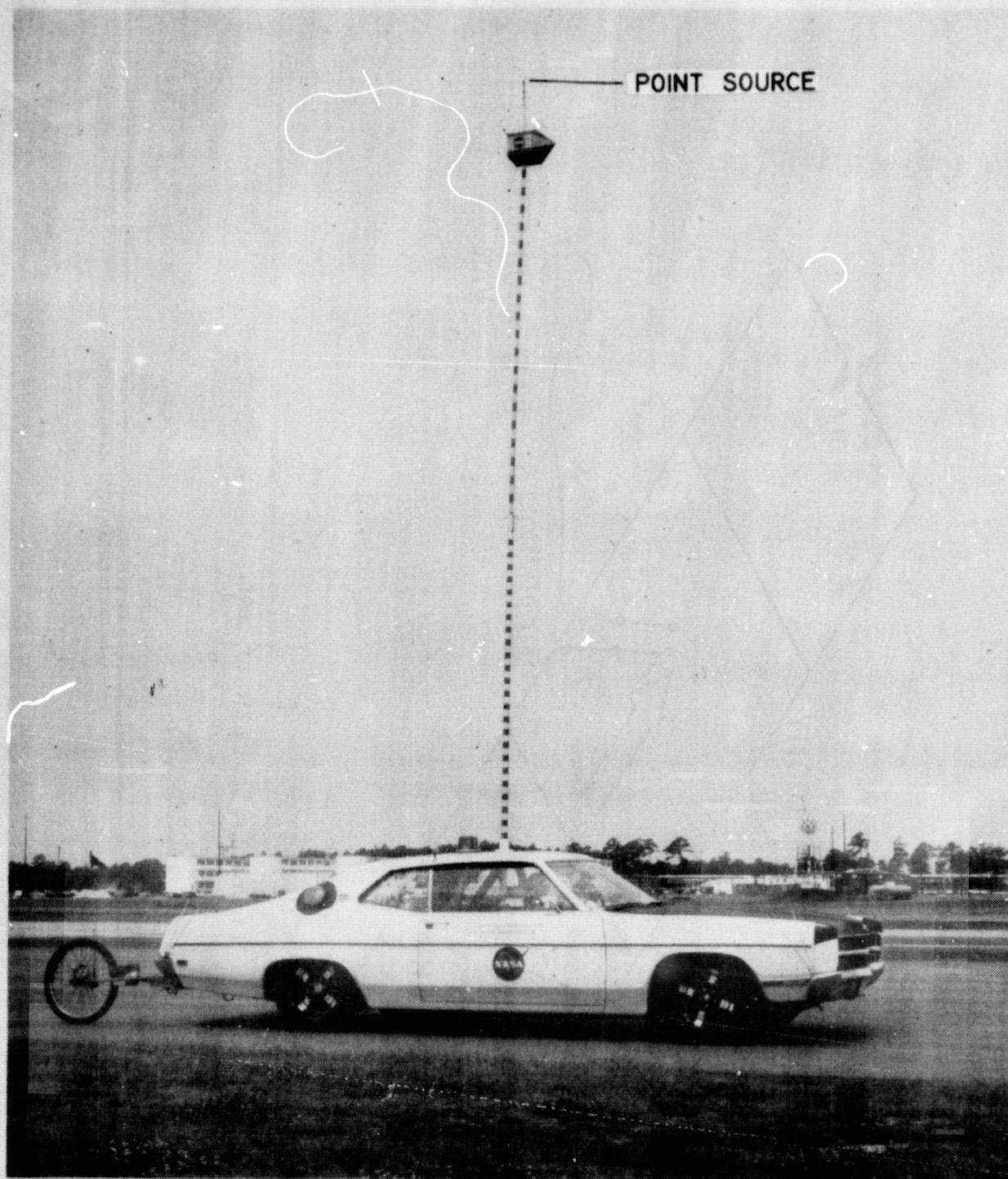


Figure 1.- Moving point source experiment.

REPRODUCIBILITY OF THE  
ORIGINAL PAGE IS POOR

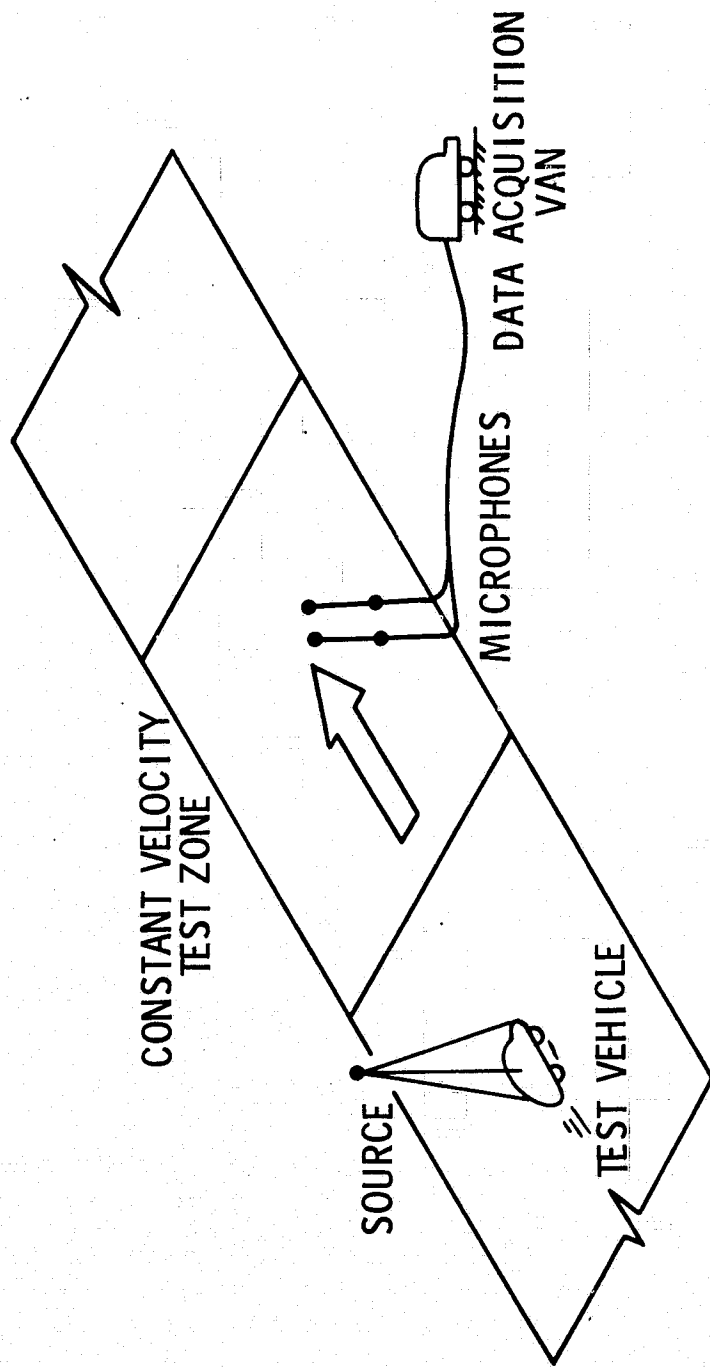


Figure 2.- Schematic of test.

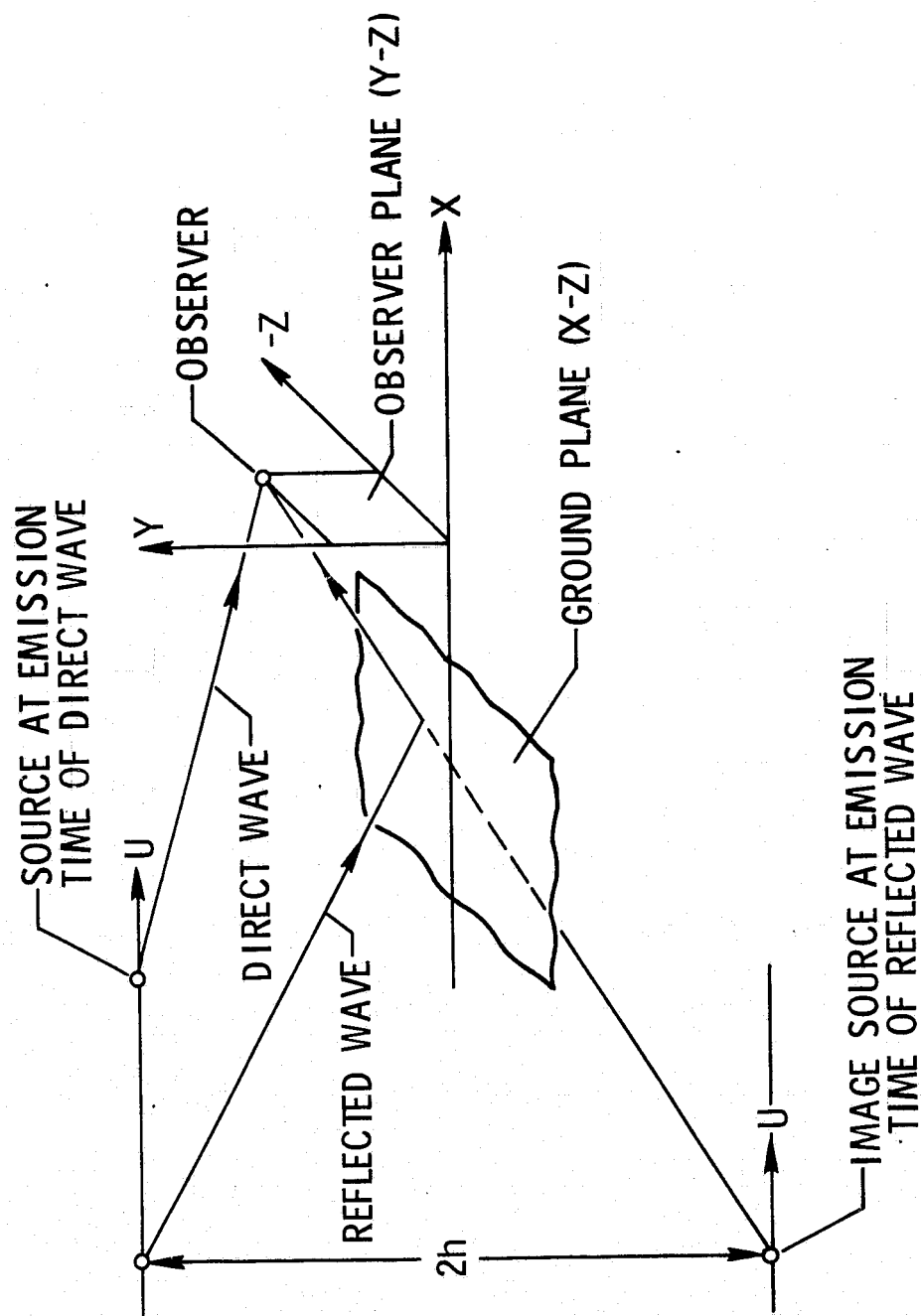


Figure 3.- Source moving at constant velocity above a ground plane.

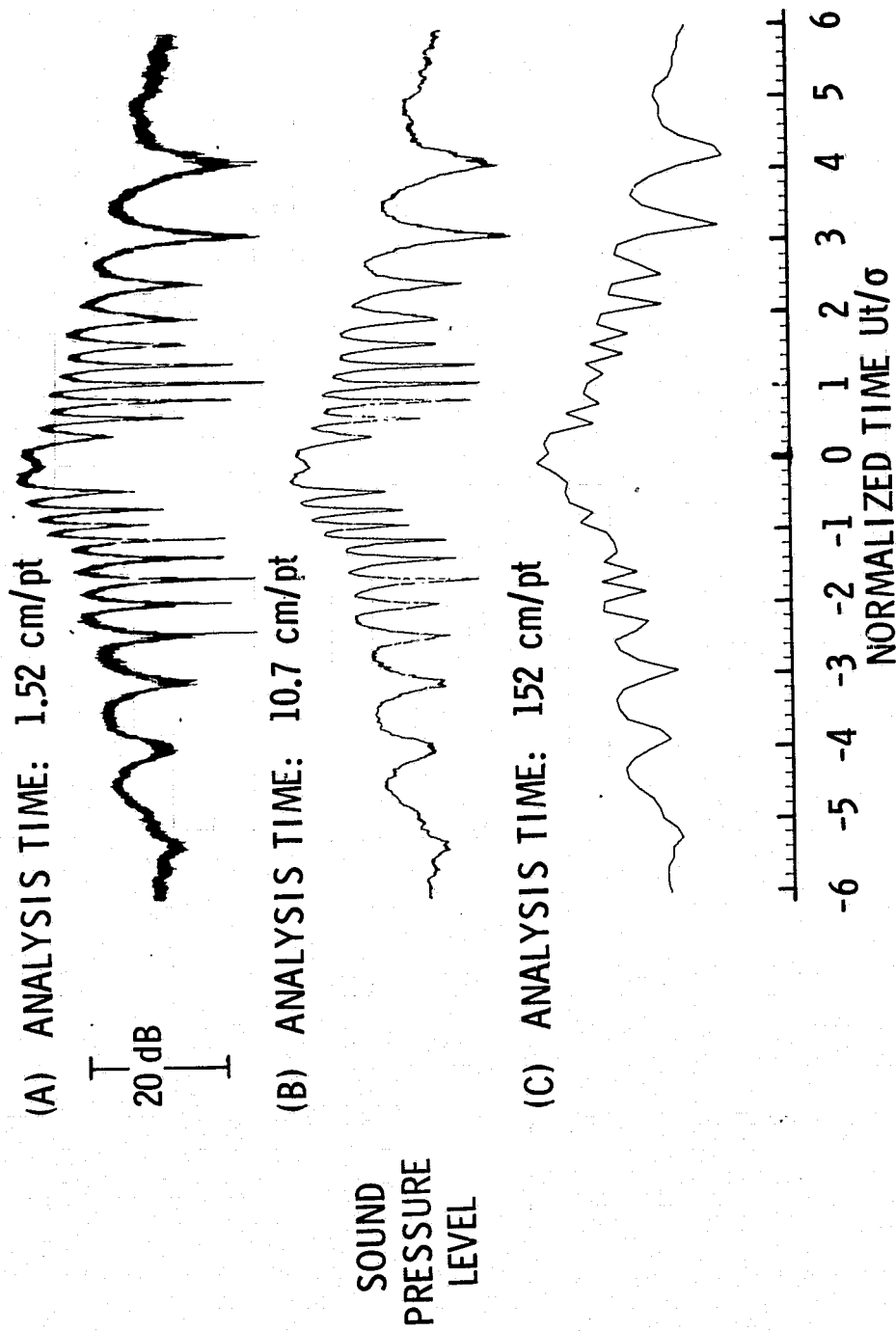


Figure 4.- Effect of analysis time on experimental noise time history. Source Frequency  $F = 1230$  Hz. Source velocity  $U = 13.4$  m/s. Observer height  $h = 3.05$  m.

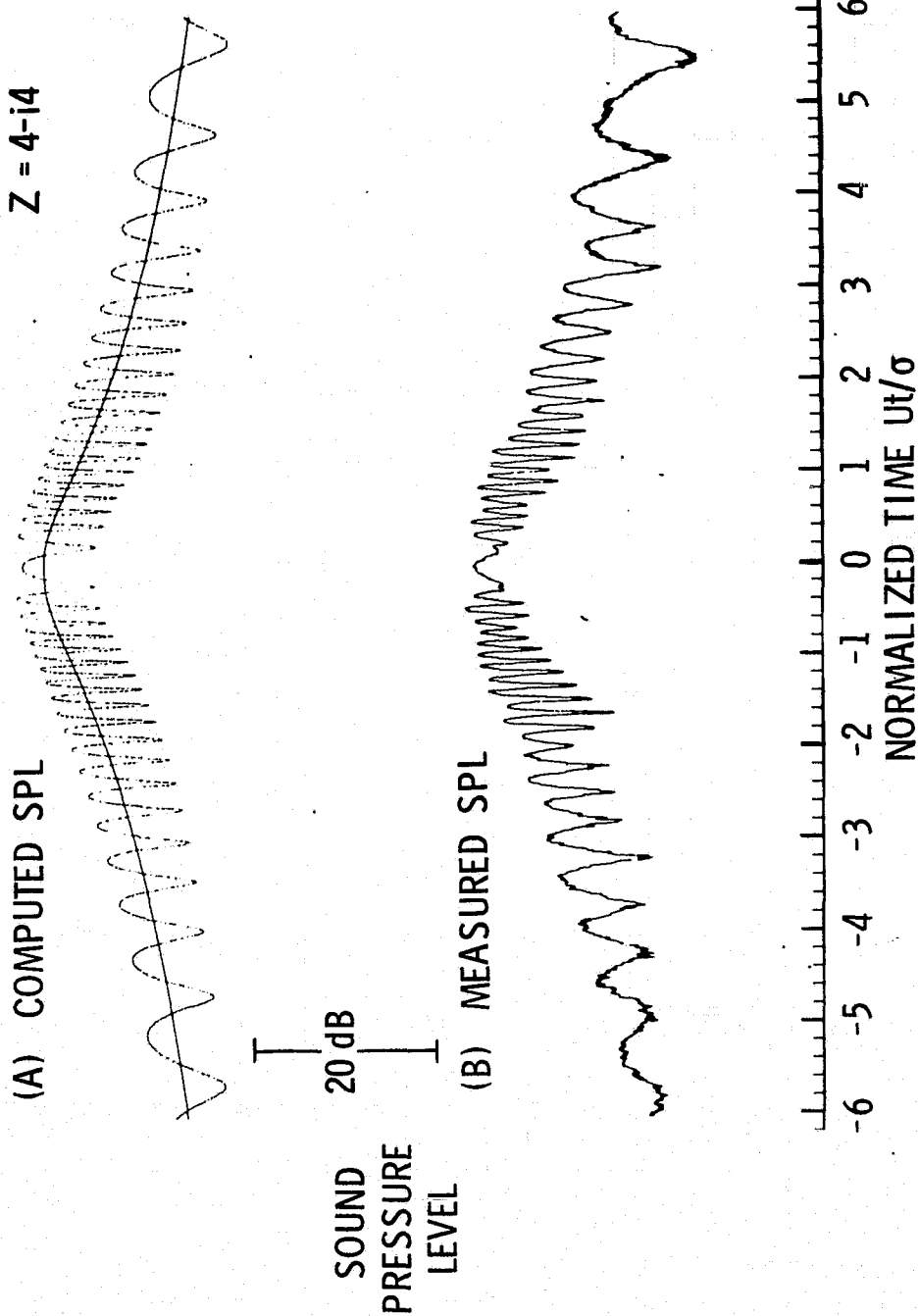


Figure 5.- Comparison of theoretical and experimental noise time histories. Source Frequency  $F = 1230$  Hz. Source velocity  $U = 13.4$  m/s. Observer height  $h = 6.10$  m. Analysis time:  $10.7$  cm/pt.



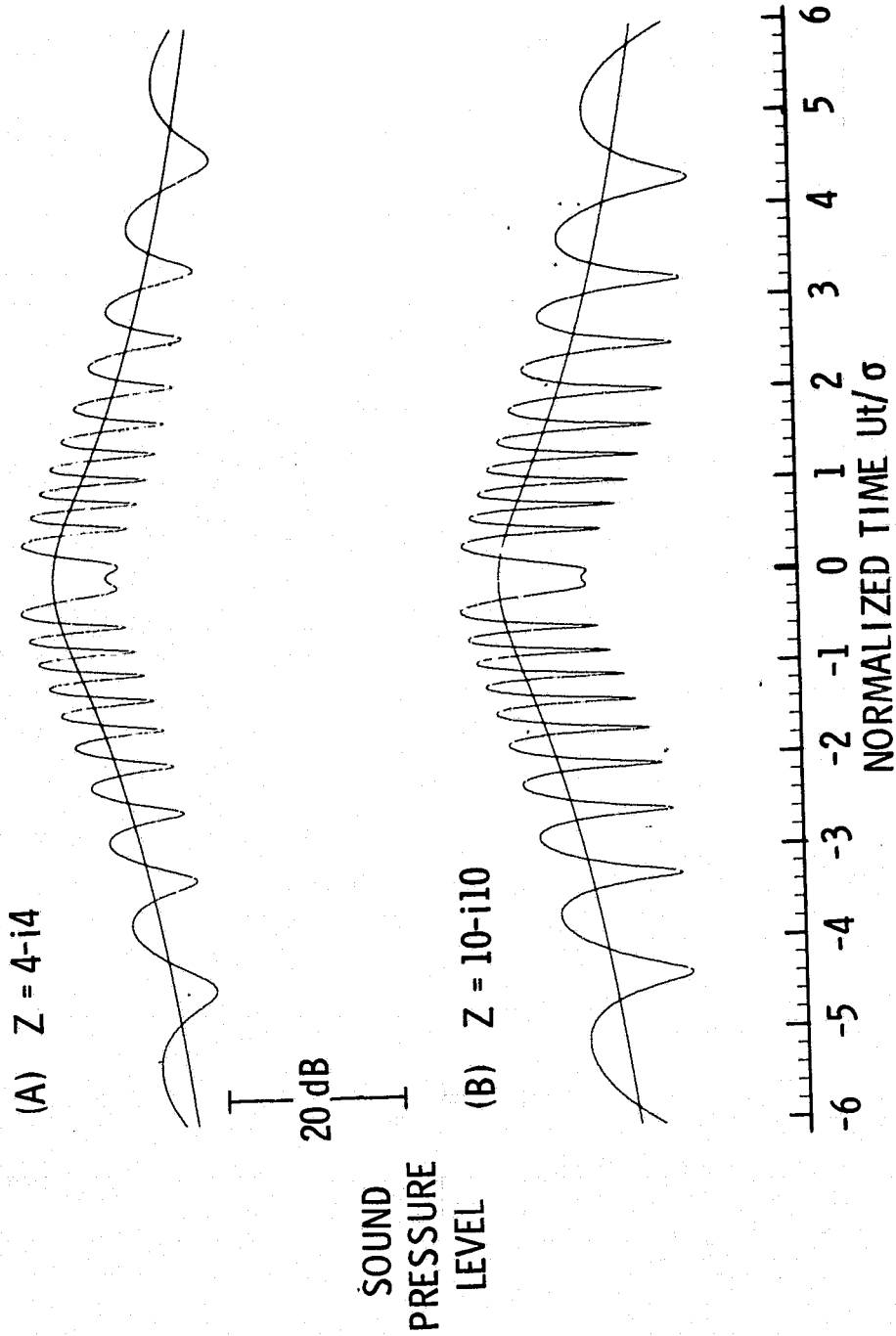


Figure 6.- Variation of computed noise-time histories with ground impedance. Source Frequency  $F = 1230$  Hz. Source velocity  $U = 13.4$  m/s. Observer height  $h = 3.05$  m.

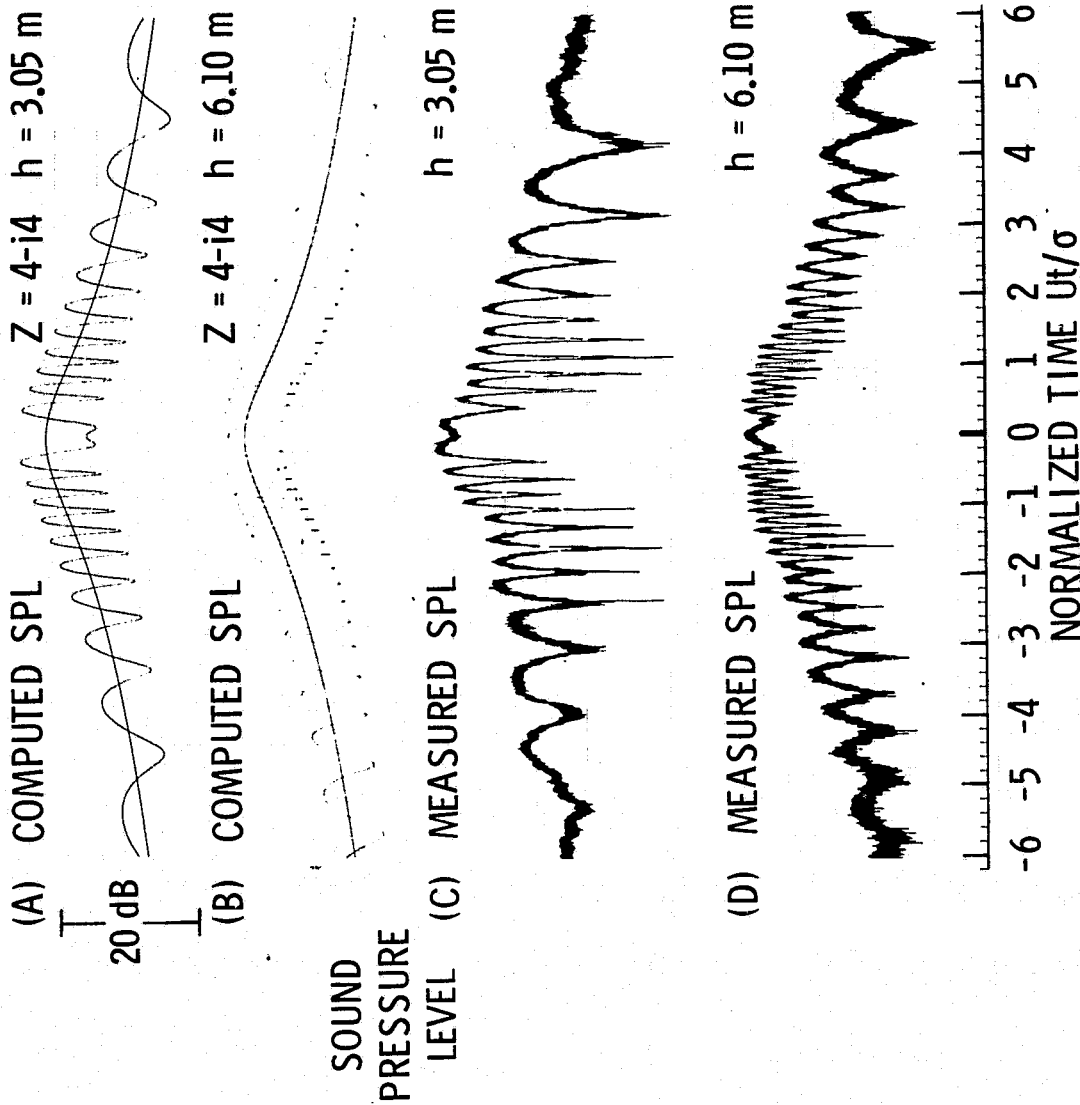


Figure 7.- Variation of computed and measured noise-time histories with observer height. Source Frequency  $F = 1230$  Hz. Source velocity =  $13.4$  m/s.

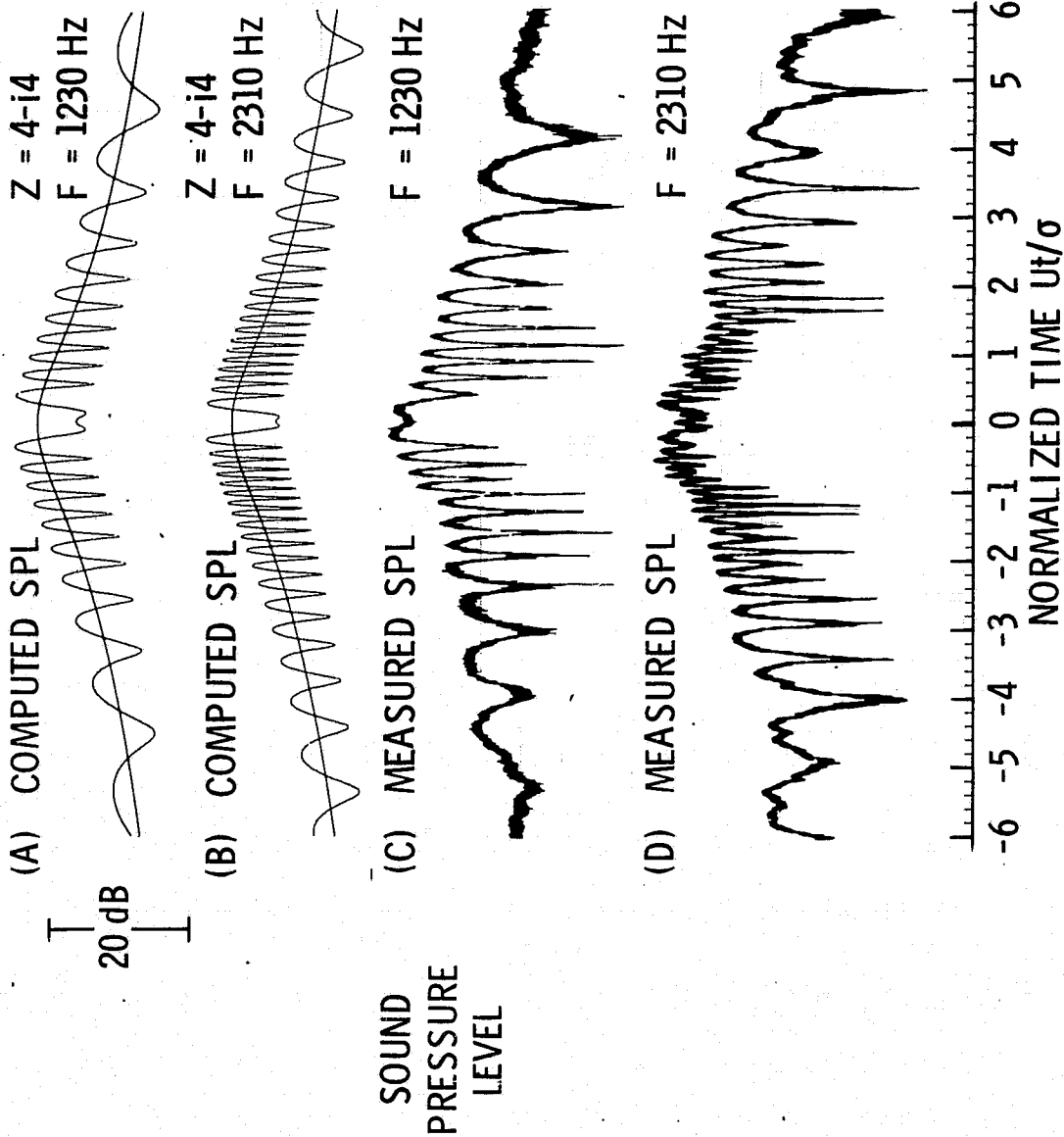


Figure 8.- Variation of computed and measured noise-time histories with frequency. Source velocity  $U = 13.4 \text{ m/s}$ . Observer height  $h = 3.05 \text{ m}$ .

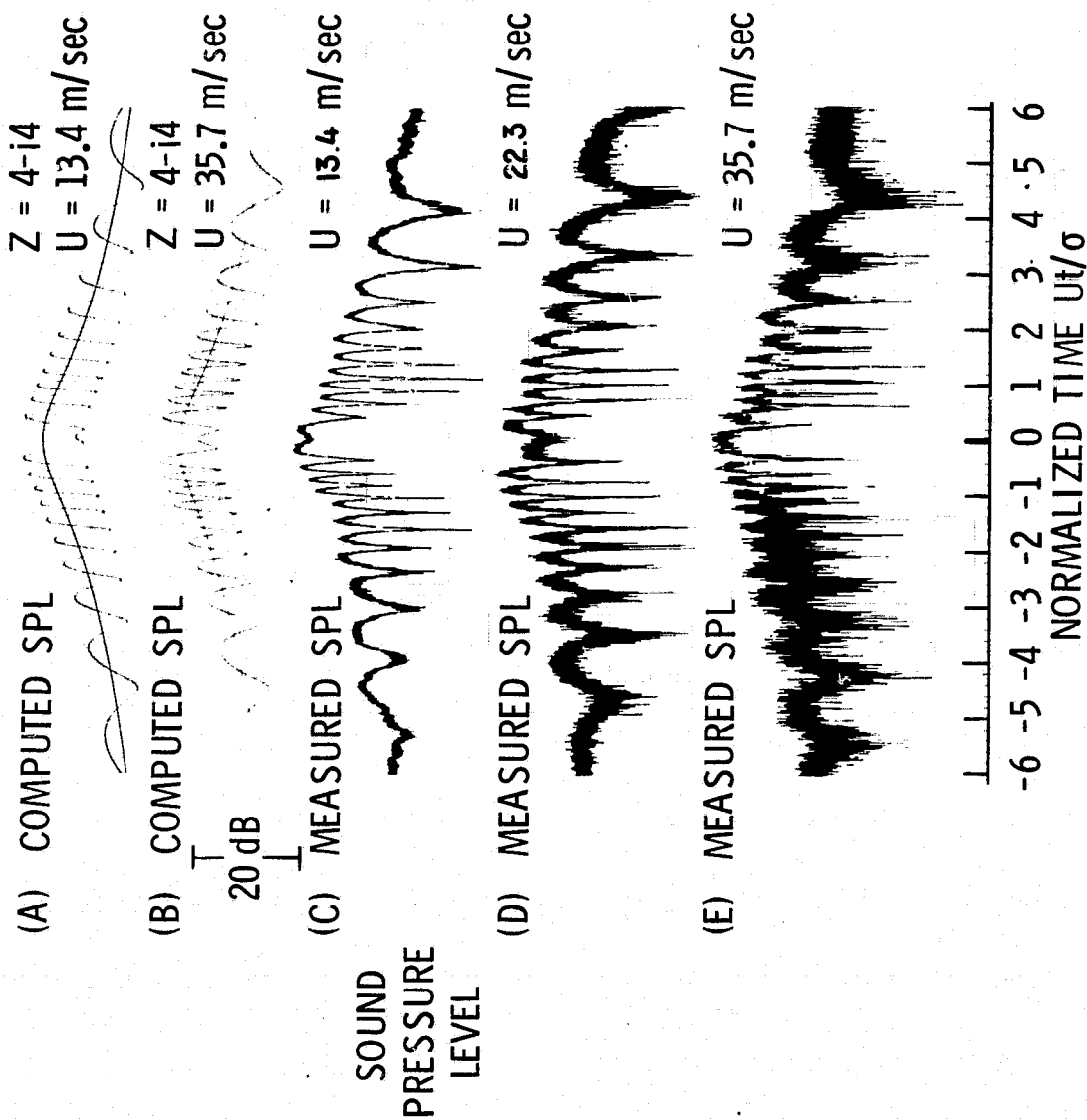


Figure 9.- Variation of computed and measured noise-time histories with source velocity. Source frequency  $F = 1230 \text{ Hz}$ . Observer height  $h = 3.05 \text{ m}$ .

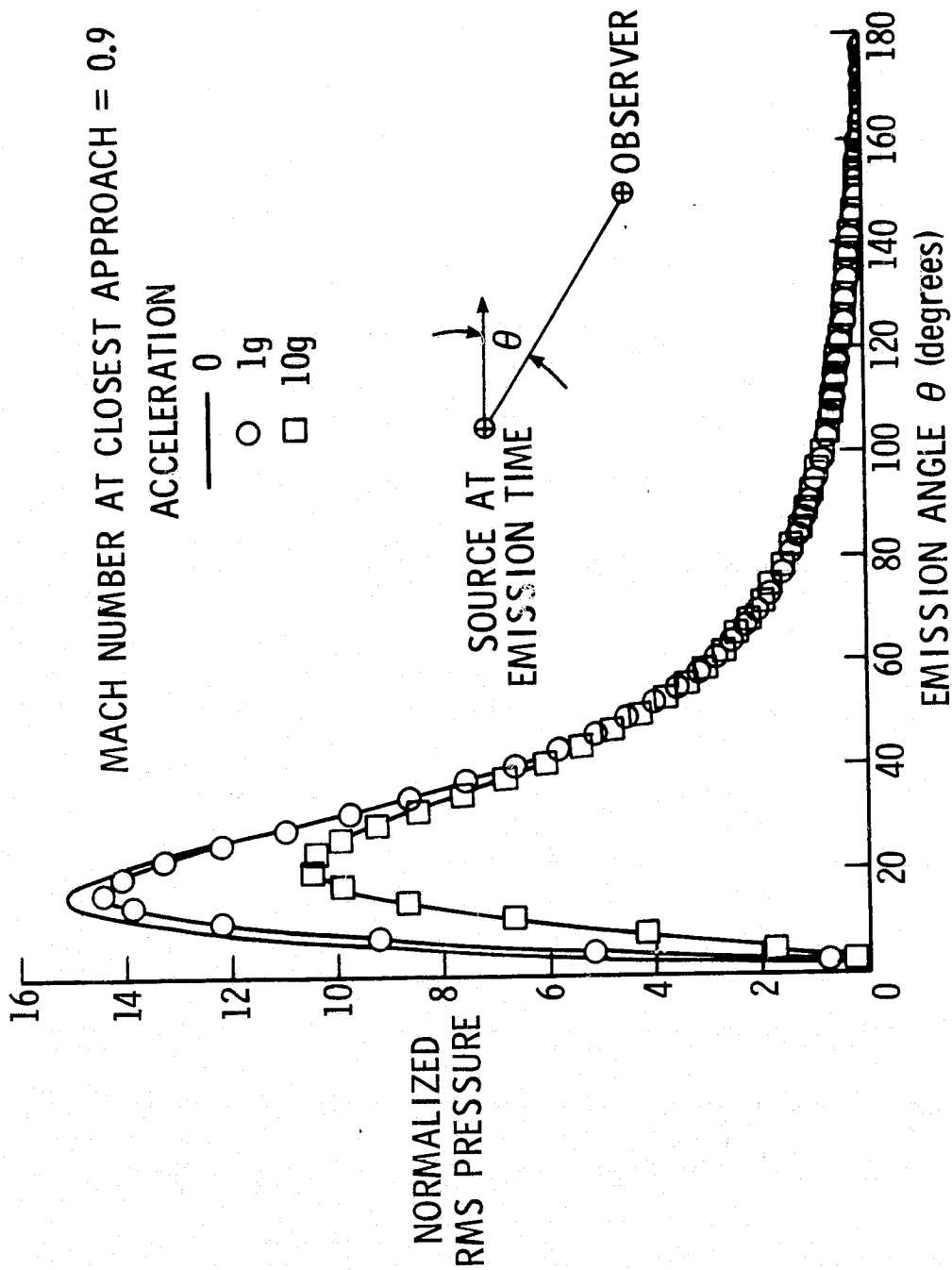


Figure 10.- Computed pressure of monopole moving with constant linear acceleration.

REPRODUCIBILITY OF THE  
ORIGINAL PAGE IS POOR